ESI

Morphological Control and Highly Efficient Catalytic Degradation Performance of Lanthanide Ferrocyanides toward Organic Dyes under Dark Ambient Conditions

Shicheng Wang, Minli Gu, Junfeng Xu, Lei Han and Fei-Yan Yi*

State Key Laboratory Base of Novel Functional Materials and Preparation Science, School of Materials Science & Chemical Engineering, Ningbo University, Ningbo, Zhejiang 315211, China.
E-mail: yifeiyan@nbu.edu.cn

Experimental part:

Materials

Ethanol, cerium nitrate hexahydrate, potassium ferrocyanide trihydrate, sodium dodecyl sulfate (SDS), sodium acetate (NaAc), polyvinyl pyrrolidone (PVP), hydrogen peroxide solution (H_2O_2, 30 wt. % in H_2O) were purchased from Aladdin Corporation. Methylene blue (MB), Rhodamine B (RhB), Methyl orange(MO) was purchased from Solarbio Corporation. All chemicals were of analytical grade and used without further purification.

Measurements

The CHN elemental analyses (%) in the solid samples were performed on a VarioEL analyzer. Energy Disperse Thermogravimetric and differential thermal analysis (TG-DTA) data were collected with a Thermal Analysis Instrument (SDT 2960, TA Instruments, New Castle, DE) at a heating rate of 10 °C/ min under air atmosphere in the Al_2O_3 crucible. Fourier-transform (FT)-IR spectra (KBr pellets) were recorded on a Nicolet 7600 FT-IR spectrophotometer in the range of 4000-500 cm^{-1}. Powder X-ray diffraction (XRD) patterns were studied on a Bruker D8 Focus diffractometer at 40 kV and 40 mA, using Cu Kα radiation Field-emission (λ = 0.15405 nm, increment = 0.02°). All UV-Vis absorption spectra were recorded using a UV spectrophotometer (UV, 3101PC, Shimadzu, Japan) at room temperature. Scanning electron microscopy (SEM) images were taken on Hitachi TM-3000 and Hitachi SU70 at an acceleration voltage of 5.0 kV. The chemical component was investigated by Energy Dispersive Spectrometer using EDAX analyzer. X-ray photoelectron spectroscopy (XPS) was recorded on a Thermo Fisher Scientific corporation Escalab 250Xi instrument

Syntheses of CePBA from CePBA-1 to CePBA-10 with different morphology.

A typical procedure is as follows. A solution of cerium nitrate hexahydrate (32.6 mg, 0.1 mmol) in 5 mL water was added dropwise to a solution of potassium ferrocyanide trihydrate (42.2 mg, 0.1 mmol) in 5 mL water under magnetic stirring. The mixture solution was further stirred for 2h. The white precipitation was centrifuged and washed several times with distilled water and absolute ethanol, and then dried at 60 °C overnight, the obtained white precipitation is labeled as

CePBA-1.

Second, when other reactive condition and order of addition keep similar as CePBA-1 except that double amount of raw material of cerium nitrate hexahydrate (65.2 mg, 0.2 mmol) and potassium ferrocyanide trihydrate (84.4 mg, 0.2 mmol) were used, he obtained white precipitation is labeled as **CePBA-2**.

Third, when the solution of cerium nitrate hexahydrate (32.6 mg, 0.1 mmol) in 5 mL water was directly poured into the solution of potassium ferrocyanide trihydrate (42.2 mg, 0.1 mmol) in 5 mL water under magnetic stirring. The mixture solution was further stirred for 2h. The obtained white precipitation is labeled as **CePBA-3**.

Fourth, when the pure aqueous solution of cerium nitrate hexahydrate (32.6 mg, 0.1 mmol) were replaced by mixed solvent system of water and ethanol with $V_{\mathrm{H2O}}/V_{\mathrm{ethanol}}$ = 1:1, other reactive conditions are similar to CePBA-3, the obtained white precipitation is labeled as **CePBA-4**.

Five, when pure ethanol solution of cerium nitrate hexahydrate (32.6 mg, 0.1 mmol) was used, the white precipitation, labeled as **CePBA-5**, was synthesized instead of CePBA-4.

Six, when PVP was introduced to the synthetic process of CePBA-3, CePBA-4, and CePBA-5, respectively, the other three white precipitations were obtained, labeled as **CePBA-6**, **CePBA-7**, and **CePBA-8**, respectively. Take the synthesis of CePBA-7 as an example, the detailed process is as follows. Typically, 0.1 mmol (42.2 mg) potassium ferrocyanide trihydrate and 250 mg polyvinyl pyrrolidone (PVP) were firstly dispersed into deionized water (DIW) (5 mL) to form a transparent solution (denoted as solution A). Then, 0.1 mmol (32.6 mg) of cerium nitrate hexahydrate was dispersed into absolute ethanol (5 mL) to form a homogeneous solution (denoted as solution B). Solution B was then poured to solution A under continuous stirring and the mixture solution was stirred for another 2 h. The precipitation was centrifuged and washed several times with distilled water and absolute ethanol respectively, and then dried at 60 °C overnight.

Seven, when SDS was utilized instead of PVP, other reactive conditions are similar to the ones of CePBA-3, as follows. 0.1 mmol (42.2 mg) potassium ferrocyanide trihydrate and 200 mg sodium dodecyl sulfate (SDS) were first dispersed into deionized water (DIW) (5 mL) to form a transparent solution (denoted as solution A). Then, 0.1 mmol (32.6 mg) of cerium nitrate hexahydrate was dispersed into DIW (5 mL) to form a homogeneous solution (denoted as solution B). Solution B was then poured into solution A directly under continuous stirring. White turbidity gradually generated and the mixture solution was further stirred for another 2h. The precipitation was centrifuged and washed several times with distilled water and absolute ethanol respectively, and then dried at 60 °C overnight. The obtained sample is labeled as **CePBA-9**.

Last, when sodium acetate (NaAC) was adopted instead of SDS, the other NaAC regulated CePBAs, labeled as **CePBA-10**, were synthesized. Its synthesized process is similar to the one of CePBA-9. Just, to investigate the influence of NaAc's concentration on the morphology of the samples, NaAc aqueous solutions with different concentration (10mg, 50mg, 100mg, 200mg, 500mg) are used in experiments.

All synthesized processes have systematically concluded in Table S1 in detail.

Dye degradation experiments.

All catalytic experiments were monitored under dark condition at room temperature. The pH value was not adjusted when the reaction was conducted. The procedure was as follows: Firstly, CePBA of 5 mg was added into 200 mL MB (20mg/L), MO (20mg/L), RhB (20mg/L) aqueous solution, respectively, and agitation for 30 min to achieve an adsorption/desorption equilibrium between the photocatalyst and dye molecules. Then 2 mL H_2O_2 solution (30 wt. %) was added into the solution. At certain time intervals, 3 mL of suspension were collected and centrifuged within 1 min to remove the catalyst. The dye value of the absorbance at the wavelength of 664 nm for MB, 553 nm for RhB, and 462 nm for MO was measured by a TU-1901 spectrometer (Beijing Purkinje General Instrument) immediately after centrifugation. The degradation efficiency was evaluated by dividing C/C_0, where C is the remained dye concentration and C_0 is the starting dye concentration. For the degradation of mixed dye solution with MB (20 mg/L) and RhB (40 mg/L), the other experimental processes are similar to above experiment procedure of degradation of single dye solution, except that catalyst of 5 mg was added into mixed dye aqueous solution of 100 mL with MB (20 mg/L) and RhB (40 mg/L).

Table S1 Syntheses of CePBA under various conditions.

Samples	Solution A: $K_4[Fe(CN)_6]$ (mmol)/solvent	Surfactant	Solution B: $Ce(NO_3)_3$ (mmol)/ solvent	mixing rate	Figure
CePBA-1	0.1 / 5 mL H_2O		0.1 / 5 mL H_2O	dropwise	Fig. 1a
CePBA-2	0.2 / 5 mL H_2O		0.2 / 5 mL H_2O	dropwise	Fig. 1b
CePBA-3	0.1 / 5 mL H_2O		0.1 / 5 mL H_2O	pour	Fig. 1c, Fig. S1
CePBA-4	0.1/ 5 mL H_2O		0.1 / 2.5 mL H_2O + 2.5 mL ethanol	pour	Fig. 1d, Fig. S2
CePBA-5	0.1 / 5 mL H_2O		0.1 / 5 mL ethanol	pour	Fig. 1e, Fig. S3
CePBA-6	0.1 / 5 mL H_2O	PVP	0.1 / 5 mL H_2O	pour	Fig. 1f, Fig. S4
CePBA-7	0.1/ 5 mL H_2O	PVP	0.1 / 2.5 mL H_2O + 2.5 mL ethanol	pour	Fig. 1g, Fig. S5
CePBA-8	0.1 / 5 mL H_2O	PVP	0.1 / 5 mL ethanol	pour	Fig. 1h, Fig. S6
CePBA-9	0.1 / 5 mL H_2O	SDS	0.1 / 5 mL H_2O	pour	Fig. S7
CePBA-10	0.1 / 5 mL H_2O	NaAC	0.1 / 5 mL H_2O	pour	Fig. S8

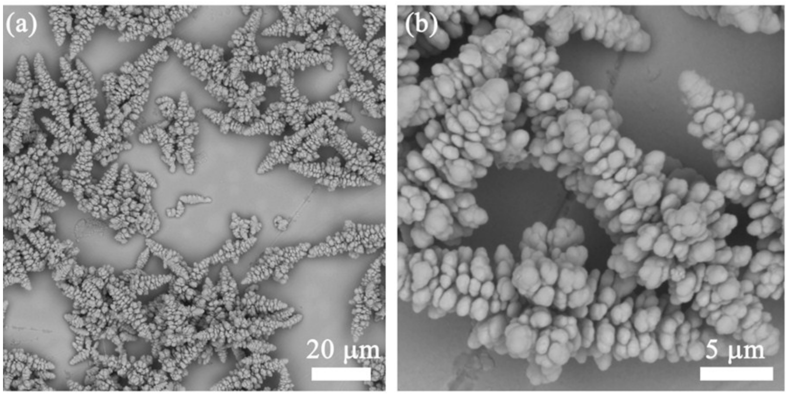

Fig. S1 SEM images of **CePBA-3** at different magnifications.

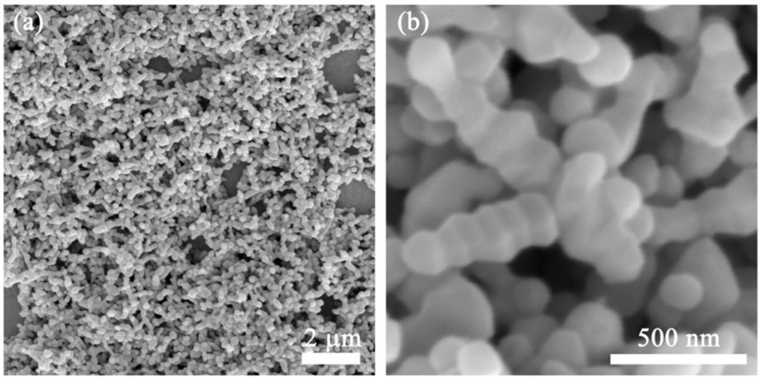

Fig. S2 SEM images of **CePBA-4** at different magnifications.

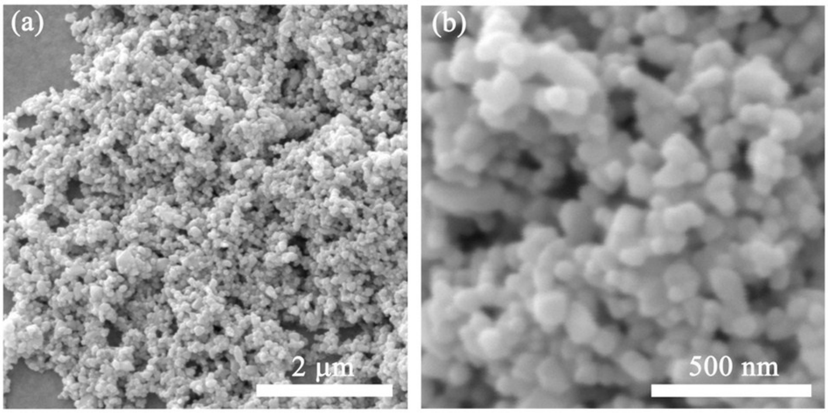

Fig. S3 SEM images of **CePBA-5** at different magnifications.

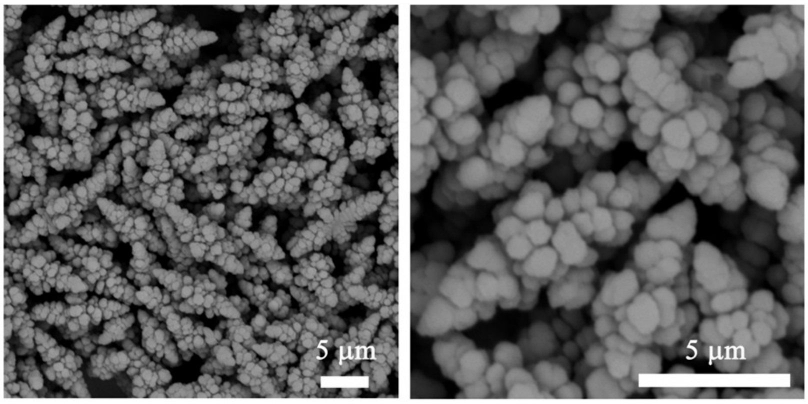

Fig. S4 SEM images of **CePBA-6** at different magnifications.

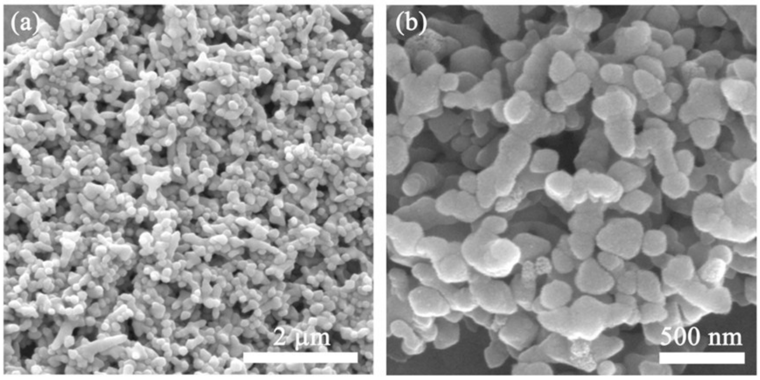

Fig. S5 SEM images of **CePBA-7** at different magnifications.

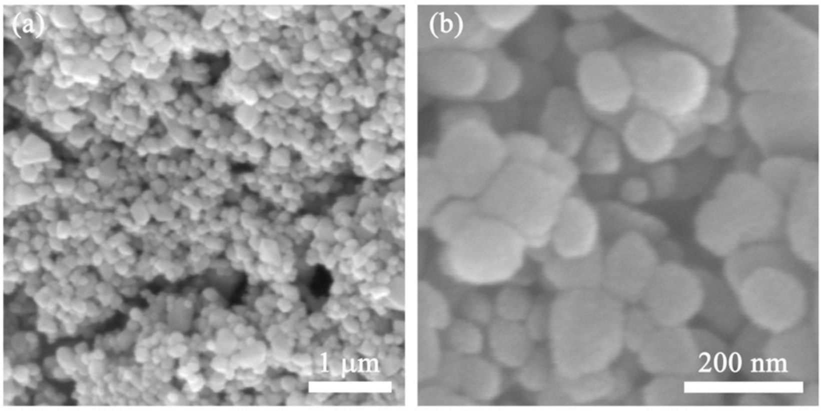

Fig. S6 SEM images of **CePBA-8** at different magnifications.

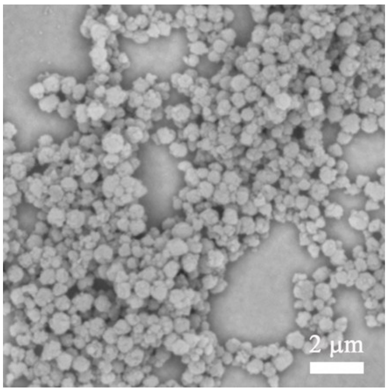

Fig. S7 SEM images of **CePBA-9**.

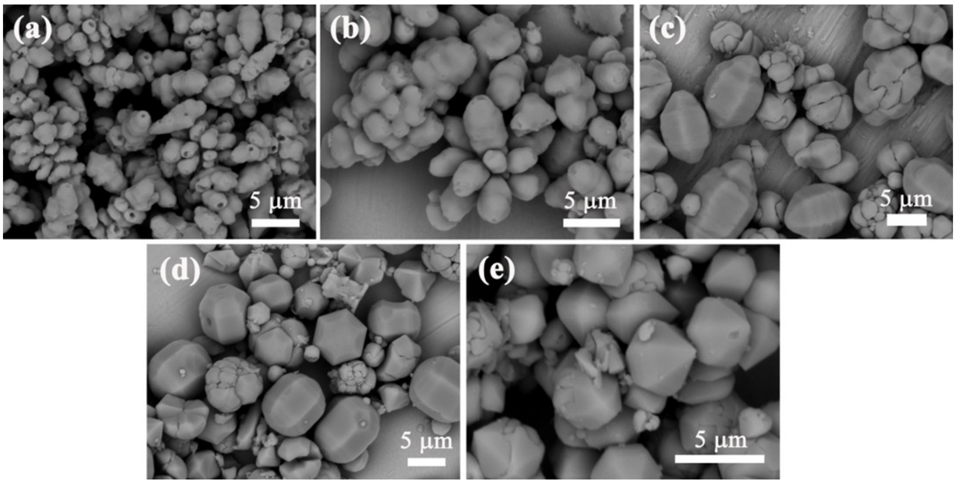

Fig. S8 SEM images of **CePBA-10** with different amount of NaAC (a for 10mg, b for 50mg, c for 100mg, d for 200mg, e for 500mg) added.

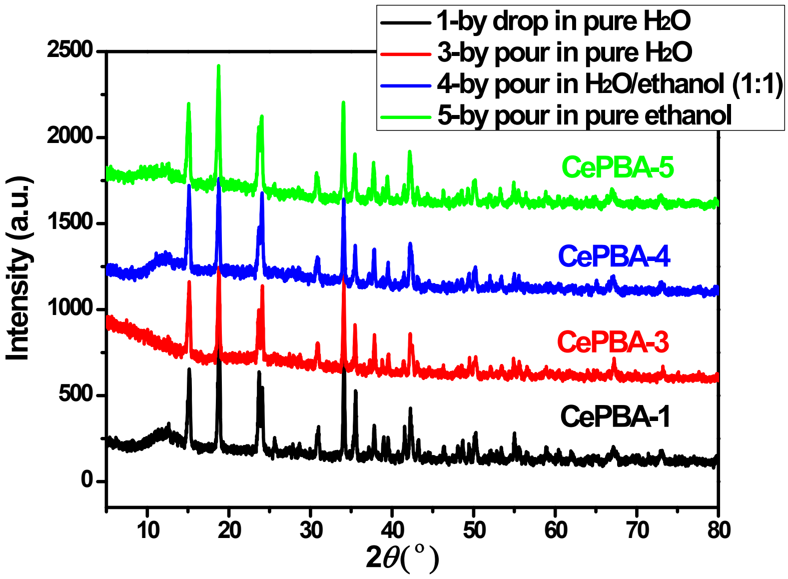

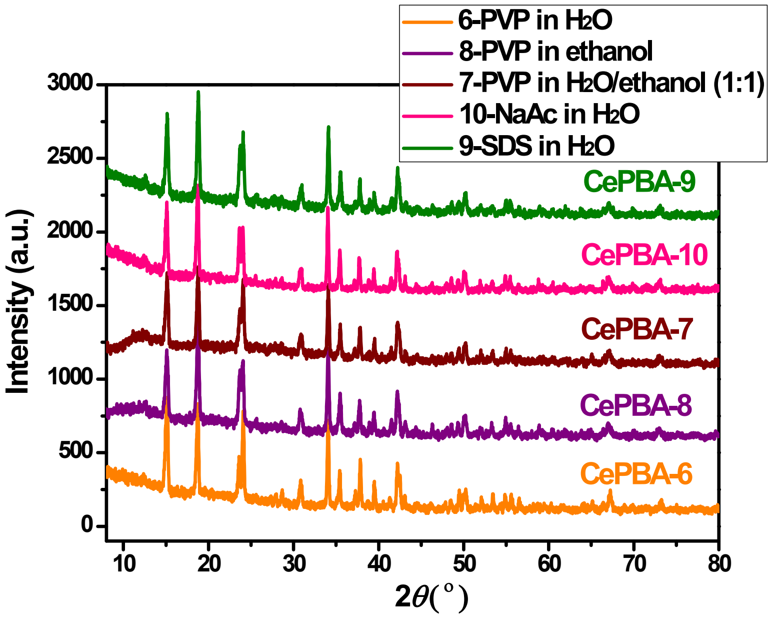

Fig. S9. The PXRD patterns of various CePBA samples based on different synthesized processes.

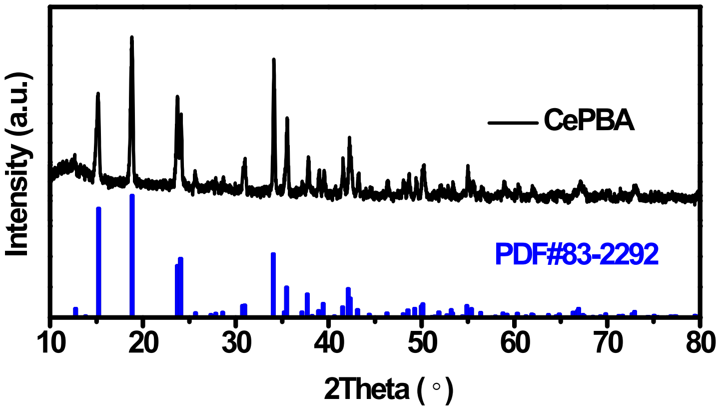

Fig. S10 PXRD pattern of CePBA we synthesized and $KCeFe(CN)_6{\cdot}4H_2O$ (PDF#83-2292).

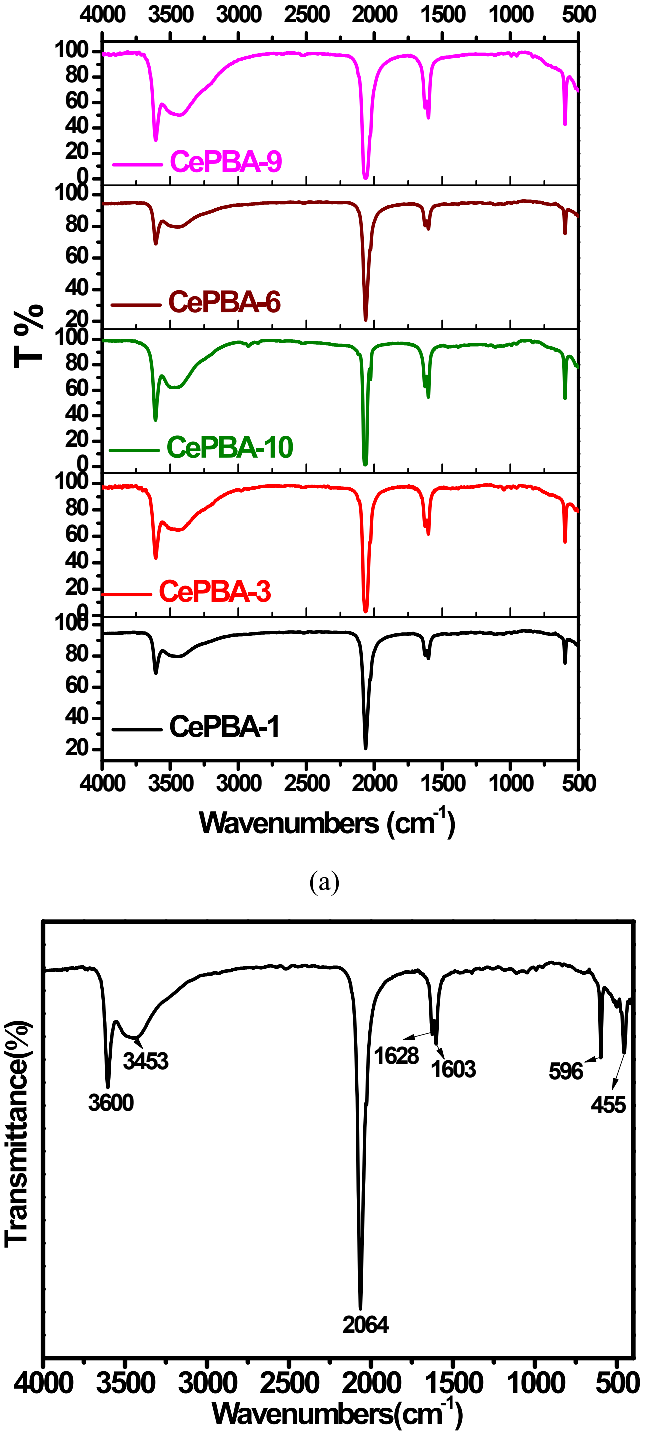

(a)

(b)

Fig. S11 FT-IR spectra of various CePBA samples.

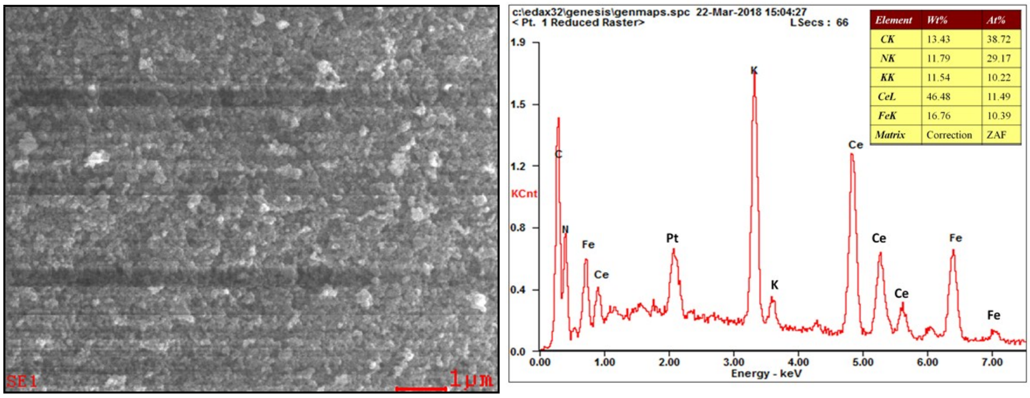

Element	*Wt%*	*At%*
CK	13.43	38.72
NK	11.79	29.17
KK	11.54	10.22
CeL	46.48	11.49
FeK	16.76	10.39
Matrix	Correction	ZAF

(a)

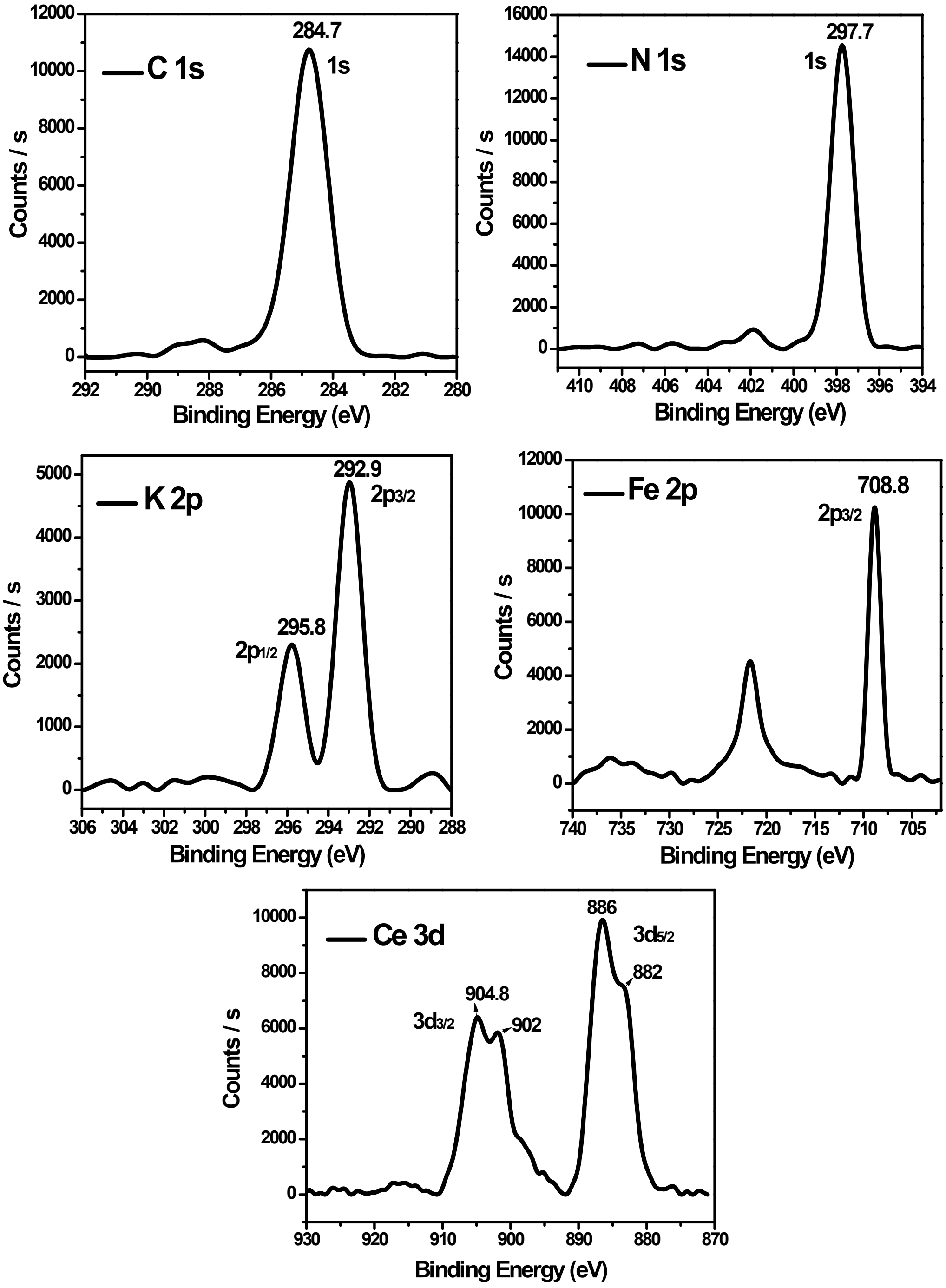

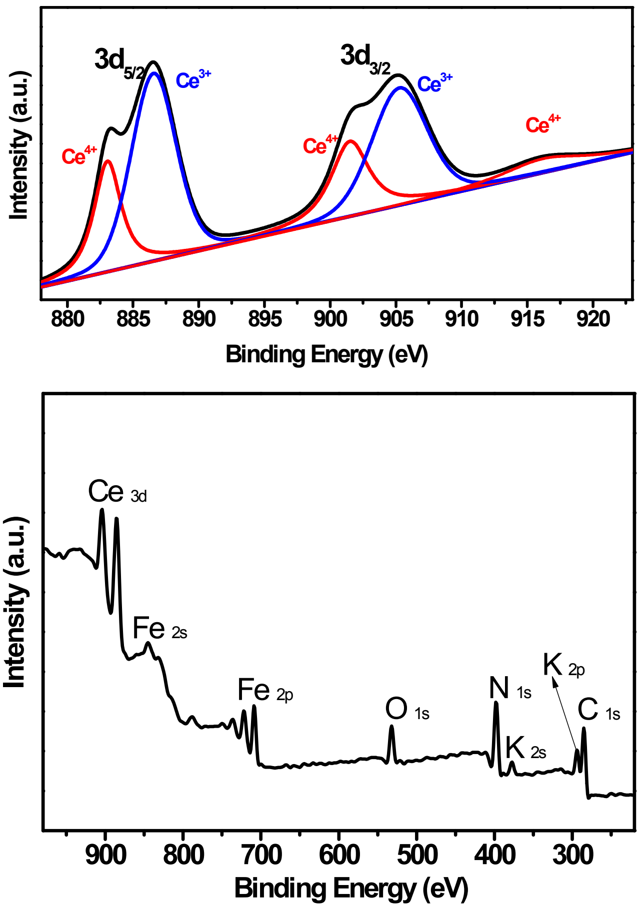

(b)

Fig. S12 (a) EDX spectrum and results of CePBA. (b) XPS results (atomic%) with 44.7% for C, 34.43% for N, 6.61% for K, 8.15% for Fe, and 6.05% for Ce.

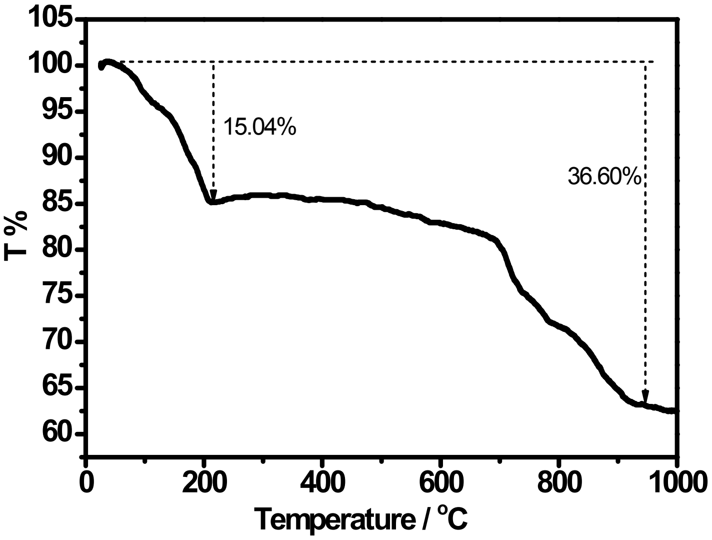

Fig. S13 TGA curve of CePBA.

As shown in Fig. S13, the TGA curve of CePBA exhibits two main weight losses. The first weight loss of 15.04% at 25-212 °C, corresponding to the loss of four water molecules per unit cell (calcd. 15%) for the formula $KCeFe(CN)_6 \cdot 4H_2O$. The desolvated framework of $KCeFe(CN)_6$ shows a long platform, demonstrating that it is still stable up to 695 °C. Then, its framework begins to collapse. The total weight loss at 976 °C is 63.4%, which is more close to the result of the mixture of $CeFeO_3$ and K_2O_2 with calculated value (64.5%) than the mixture of CeO_2, Fe_2O_3 and K_2O_2, with the calculated value (66.3%).

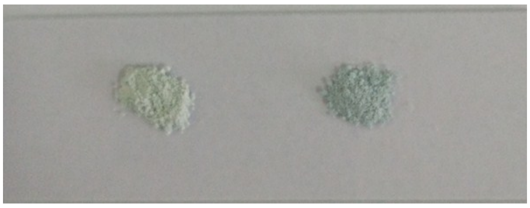

Fig. S14 The images of CePBA sample (left, freshly prepared) and CePBA sample (right, after exposure in air for 1 week).

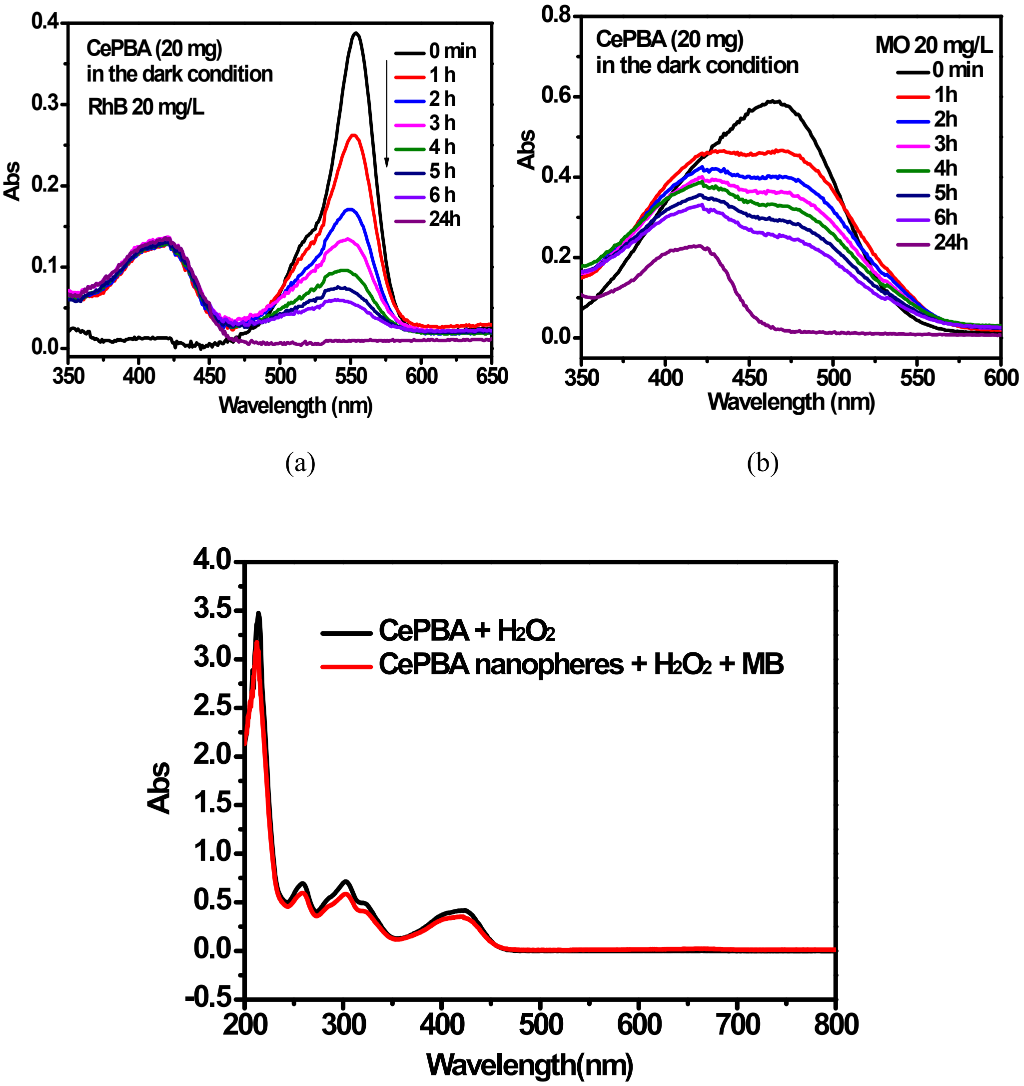

(a) (b)

(c)

Fig. S15 Time-dependent UV-vis absorption spectra of CePBA for degrading of RhB (a), and MO (b) in the dark environment. (c) UV-vis absorption spectra of CePBA aqueous solution with H_2O_2 and after degrading MB with H_2O_2.

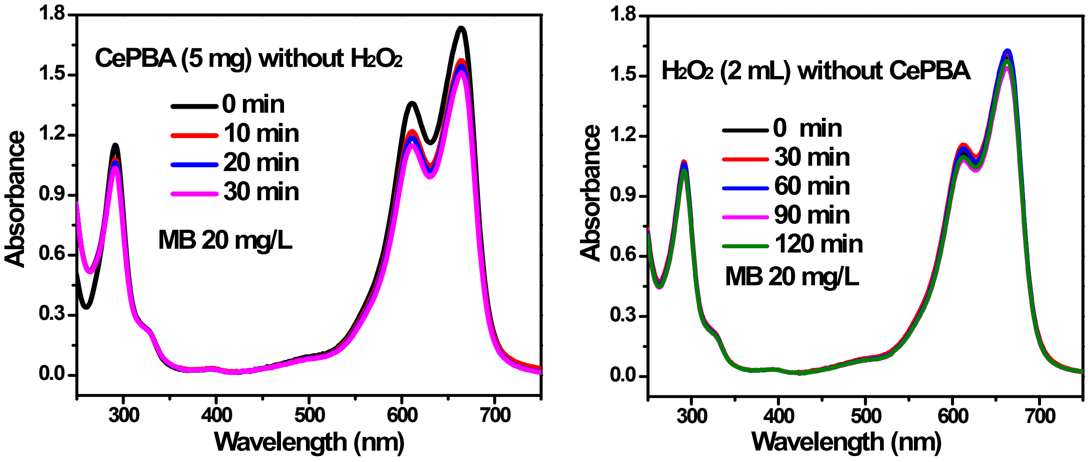

Fig. S16 The degradation of MB solution (20 mg/L, 200 mL) in the presence of individual CePBA (5 mg) or H_2O_2 (2 mL), respectively.

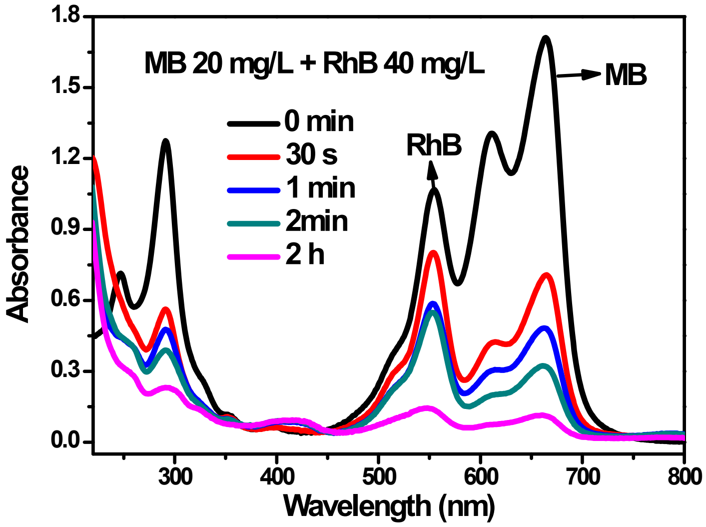

Fig. S17 The catalytic performance of CePBA-8 toward mixed dye aqueous solution of MB (20 mg/L) and RhB (40 mg/L).

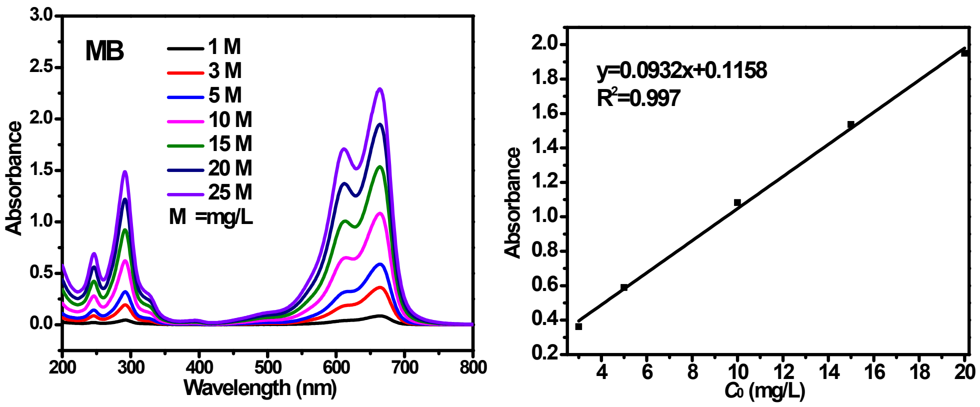

(a)

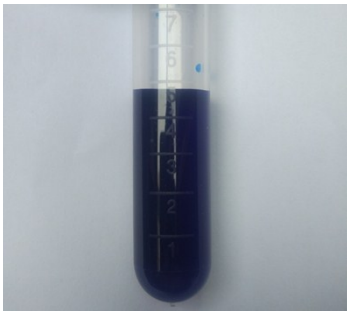

(b)

Fig. S18 (a) UV-vis spectra of aqueous solutions of MB dye with different concentrations, as well as the absorbed intensity (black dots) of MB dyes in different concentrations (C_0 = mg/L). The black solidline are the best linear fit. (b) The image of aqueous solution of MB of 150 mg/L.

Table S2 Comparative details of degradation effiency and reaction coditions of reported catalysts and this work toward degradation of MB.

Catalyst	Reaction conditions	Degradation performance	Ref.
RGO-CeO_2 NCs	Conditions: UV light, ambient Input oxidant: none Catalyst loading: 30 mg	Concentration of dye: 1×10^{-5} M (80 mL) Efficiency: 87% Time: 90 min	1
CeO_2/ZnO microstructures	Conditions: UV light, ambient Input oxidant: none Catalyst loading: 10 mg	Concentration of dye: 10 mg/L (100 mL) Efficiency: 67.4% Time: 150 min	2
Self-assembled GO with Fe-aminoclay	Conditions: minimal light exposure, ambient Input oxidant: 1.0 wt% of H_2O_2 Catalyst loading: 610 mg/L	Concentration of dye: 20mg/L (20 mL) Efficiency: ~100% Time: 4 h	3
Fe_2O_3@SiO_2	Conditions: dark, ambient Input oxidant: 18 g/L H_2O_2 Catalyst loading: 10 mg	Concentration of dye: 50 mg/L (20 mL) Efficiency: 90% Time: 7h	4
ZnO_2/polypyrrole	Conditions: dark/visible light/UV light, ambient Input oxidant: none Catalyst loading: 1.6 g/L	Concentration of dye: 5 ppm Efficiency: 83%/95%/100% Time: 20 min	5
Ag_3PO_4/CeO_2 composites	Conditions: visible light/UV light, ambient Input oxidant: none Catalyst loading: 30 mg	Concentration of dye: 10 mg/L (80 mL) Efficiency: ~98%/98.9% Time: 60min/6min	6
Iron-cerium mixed oxides	Conditions: sun light, ambient Input oxidant: none Catalyst loading: 40 mg	Concentration of dye: 100 ppm (20 mL) Efficiency: 93% Time: 4 h	7
CeO_2 spheres	Conditions: sun light, ambient Input oxidant: none	Concentration of dye: 20 mg/L (400 mL) Efficiency: over 80%	8

	Catalyst loading: 100 mg	Time: within 120 min	
Fe^0-Fe_3O_4-RGO	Conditions: pH=3.00, ambient Input oxidant: 0.8 mmol/L H_2O_2 Catalyst loading: 100 mg/L	Concentration of dye: 50 mg/L Efficiency: 98.0% Time: within 60 min	9
Porous nitrogen-doped carbon microspheres	Conditions: pH=6.30, ambient Input oxidant: 1.0 g/L Oxone Catalyst loading: 5 mg	Concentration of dye: 100 mg/L (50 mL) Efficiency: 85.0%/almost 100.0% Time: 2 min/10 min	10
α-Fe_2O_3	Conditions: visible light, ambient Input oxidant: none Catalyst loading: 50 mg	Concentration of dye: 5 mg/L (50 mL) Efficiency: 38% Time: 180 min	11
(Yb,N)-TiO_2	Conditions: visible light, ambient Input oxidant: none Catalyst loading: 150 mg	Concentration of dye: 10 mg/L (50 mL) Efficiency: 93.55% Time: 5h	12
GO/Mn_3O_4	Conditions: room temperature Input oxidant: 5.0 wt% H_2O_2 Catalyst loading: 10 mg	Concentration of dye: 50 mg/L (50 mL) Efficiency: 100% Time: within 200 min	13
$BiVO_4$/Ag_3VO_4 heterojunction	Conditions: visible light, ambient Input oxidant: none Catalyst loading: 100 mg	Concentration of dye: 10 mg/L (100 mL) Efficiency: 64.3% Time: 40 min	14
WO_3-ZnO	Conditions: visible light, ambient Input oxidant: none Catalyst loading: 50 mg	Concentration of dye: 10 ppm (50 mL) Efficiency: 93% Time: 120 min	15
CuO nanoleaves	Conditions: UV light, ambient Input oxidant: none Catalyst loading: 5 mg	Concentration of dye: 15 mg/L (100 mL) Efficiency: 89% Time: 180 min	16
TiO_2/CNSAC	Conditions: sun light, ambient Input oxidant: none Catalyst loading: 20 mg/L	Concentration of dye: 10 mg/L (100 mL) Efficiency: 96.35% Time: 120 min	17
SiO_2/TiO_2	Conditions: sun light, ambient Input oxidant: none Catalyst loading: unknown	Concentration of dye: 10 mg/L Efficiency: 97.7% Time: 30 min	18
Co_3O_4/ZnO NRs	Conditions: UV light, ambient Input oxidant: none Catalyst loading: covered on Ni foil	Concentration of dye: 10 mg/L (50 mL) Efficiency: 100% Time: 96 h	19
ZnO-	Conditions: UV light, ambient	Concentration of dye: 10 mg/L (30 mL)	20

NPs/RGO	Input oxidant: none Catalyst loading: 10 mg	Efficiency: 99.5% Time: 180 min	
Ag-TiO_2	Conditions: UV light, ambient Input oxidant: none Catalyst loading: 2 mg	Concentration of dye: 1×10^{-5} M (12 mL) Efficiency: 71% Time: 60 min	21
Ag_2WO_4@g-C_3N_4	Conditions: simulated solar light Input oxidant: none Catalyst loading: 1.25 g/L	Concentration of dye: 10 ppm (50 mL) Efficiency: 100% Time: 120 min	22
Fe_2O_3/TiO_2	Conditions: UV light/visible light, ambient, pH=4 Input oxidant: none Catalyst loading: 2 g	Concentration of dye: 25 mg/L (80 mL) Efficiency: 83%/88% Time: 5 h	23
$CoFe_2O_4$/g-C_3N_4	Conditions: visible light, ambient Input oxidant: 6.25 mL/L of 30% H_2O_2 Catalyst loading: 20 mg/L	Concentration of dye: 10 mg/L (80 mL) Efficiency: 97.3% Time: 3 h	24
AgNPs	Conditions: UV light, ambient Input oxidant: none Catalyst loading: 8 mg	Concentration of dye: 15 mg/L (70 mL) Efficiency: 96% Time: 80 min	25
paper mill sludge-derived Fe-loading nanocomposite	Conditions: ambient, pH=4 Input oxidant: 2 mL/L of 30% H_2O_2 Catalyst loading: 100 mg	Concentration of dye: 50 mg/L (100 mL) Efficiency: 93.3% Time: 80 min	26
rGO-CdO	Conditions: UV light, ambient Input oxidant: none Catalyst loading: 50 mg	Concentration of dye: 1×10^{-5} M (50 mL) Efficiency: 80% Time: 110 min	27
$Ag_3PO_4/ZnFe_2O_4$	Conditions: visible light, ambient Input oxidant: none Catalyst loading:100 mg	Concentration of dye: 5 mg/L (100 mL) Efficiency: 100% Time: 60 min	28
RGO/meso-TiO_2/AuNPs	Conditions: visible light, ambient Input oxidant: none Catalyst loading: 10 mg	Concentration of dye: 30 mg/L (70 mL) Efficiency: almost 100% Time: 240 min	29
3-D CuS caved superstructures	Conditions: dark, ambient Input oxidant: 1 wt% H_2O_2 Catalyst loading: 10 mg	Concentration of dye: 3×10^{-5} M (10 mL) Efficiency: 96.6% Time: 30 min	30
CePBA	**Conditions: dark, ambient** **Input oxidant: 0.3 wt%**	**Concentration of dye: 120 mg/L (100 mL)**	**This work**

	H_2O_2 **Catalyst loading: 5 mg**	**Efficiency: 100%** **Time: 30 seconds**	

References:

(1) K. Huang, Y. H. Li, S. Lin, C. Liang, X. Xu, Y. F. Zhou, D.Y. Fan, H. J. Yang, P. L. Lang, R. Zhang, Y.G. Wang and M. Lei, *Mater. Lett.*, 2014, **124**, 223-226.

(2) I-T. Liu, M.-H. Hon and L. G. Te, *Ceram. Int.*, 2014, **40**, 4019-4024.

(3) Y.-C. Lee, S.-J. Chang, M.-H. Choi, T.-J. Jeon, T. Ryud and Y. S. Huh, *Appl. Catal. B: Environ.*, 2013, **142-143**, 494-503.

(4) Z.-M. Cui, Z. Chen, C.-Y. Cao, L. Jiang and W.-G. Song, *Chem. Commun.*, 2013, **49**, 2332-2334.

(5) L. Prasanna, V. Rajagopalan, *Sci. Rep.*, 2016, **6**, 38606-38616.

(6) Z.-M. Yang, G.-F. Huang, W.-Q. Huang, J.-M. Wei, X.-G. Yan, Y.-Y. Liu, C. Jiao, Z. Wan and A. Pan, *J. Mater. Chem. A*, 2014, **2**, 1750-1756.

(7) G. K. Pradhan and K. M. Parida, *Int. J. Eng. Sci. Tec.*, 2010, **2**, 53-65.

(8) J. Qian, Z. Chen, C. Liu, X. Lu, F. Wang and M. Wang, *Mat. Sci. Semicon. Proc.*, 2014, **25**, 27-33.

(9) B. Yang, Z. Tian, L. Zhang, Y. Guo and S. Yan, *J. Water Proc. Eng.*, 2015, **5**, 101-111.

(10) N. Wang, W. Ma, Z. Ren, Y. Du, P. Xu and X. Han, *J. Mater. Chem. A*, 2018, **6**, 884-895.

(11) H. Liang, K. Liu and Y. Ni, *Mater. Lett.*, 2015, **159**, 218-220.

(12) J. Zhang, L. J. Xu, Z. Q. Zhu and Q. J. Liu, *Mater. Res. Bull.*, 2015, **70**, 358-364.

(13) Y. Li, J. Qua, F. Gao, S. Lv, L. Shi, C. He and J. Sun, *Appl. Catal. B: Environ.*, 2015, **162**, 268-274.

(14) M. Yan, Y. Wu, Y. Yan, X. Yan, F. Zhu, Y. Hua and W. Shi, *ACS Sustainable Chem. Eng.,* 2016, **4**, 757−766.

(15) S. Adhikari, D. Sarkar and G. Madras, *RSC Adv*., 2015, **5**, 11895-11904.

(16) S. Sonia, S. Poongodi, P. Suresh Kumar, D. Mangalaraj, N. Ponpandian, C. Viswanathan, *Mat. Sci. Semicon. Proc*., 2015, **30**, 585-591.

(17) S. Ragupathy, K. Raghu and P. Prab, *Spectrochim. Acta A*, 2015, **138**, 314-320.

(18) L. Wu, Y. Zhou, W. Nie, L. Song and P. Chen, *Appl. Surf. Sci.*, 2015, **351**, 320-326.

(19) C. Dong, X. Xiao, G. Chen, H. Guan and Y. Wang, *Mater. Chem. Phys.*, 2015, **155**, 1-8.

(20) M. Azaranga, A. Shuhaimia, R. Yousefic, A. M. Golsheikha and M. Sookhakian, *Ceram. Int.*, 2014, **40**, 10217-10221.

(21) I. H. Chowdhury, S. Ghosh and M. K. Naskar, *Ceram. Int.*, 2016, **42**, 2488-2496.

(22) K. Vignesh and M. Kang, *Mat. Sci. Eng. B*, 2015, **199**, 30-36.

(23) R. Li, Y. Jia, N. Bu, J. Wu and Q. Zhen, *J. Alloy. Compd.*, 2015, **643**, 88-93.

(24) S. Huang, Y. Xu, M. Xie, H. Xu, M. He, J. Xia, L. Huang and H. Li, *Colloid. Surface A*, 2015, **478**, 71-80.

(25) K. Tahir, S. Nazir, B. Li, A. U. Khan, Z. U. H. Khan, A. Ahmad and F. U. Khan, *Sep. Purif. Technol.*, 2015, **150**, 316-324.

(26) G. Zhou, F. Fang, Z. Chen, Y. He, H. Sun and H. Shi, *Catal. Commun.*, 2015, **62**, 71-74.

(27) S. Kumar, A. K. Ojha and B. Walkenfort, *J. Photoch. Photobio. B*, 2016, **159**, 111-119.

(28) M. Ge, Y. Chen, M. Liu and M. Li, *J. Environ. Chem. Eng*., 2015, **3**, 2809-2815.

(29) Y. Yang, Z. Ma, L. Xu, H. Wang and N. Fu, *Appl. Surf. Sci.*, 2016, **369**, 576-583.

(30) Q. W. Shu, J. Lan, M. X. Gao, J. Wang and C. Z. Huang, *CrystEngComm*, 2015, **17**, 1374-1380.

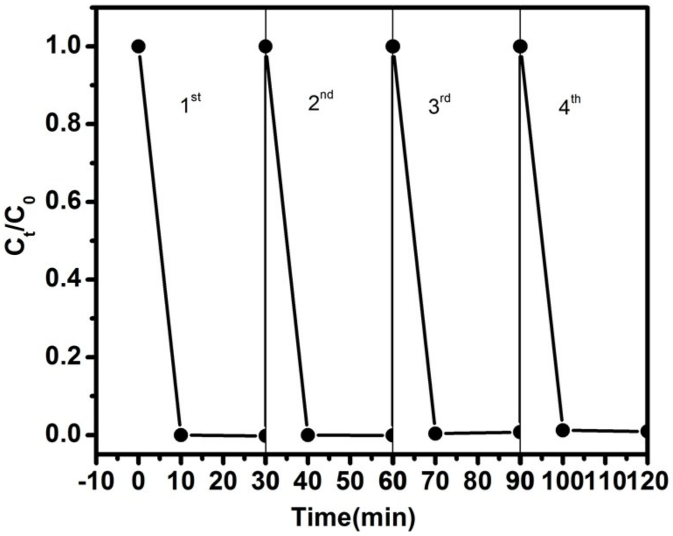

Fig. S19 Reusability of CePBA as a heterogeneous catalyst toward the degradation of MB (20 mg/L).

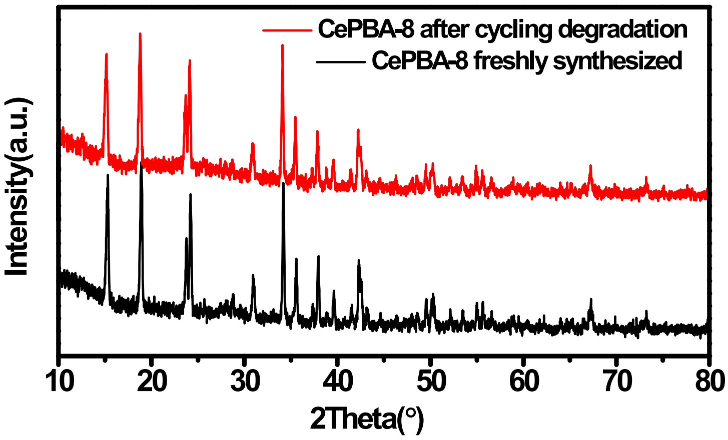

Fig. S20 The PXRD pattern of CePBA-8 sample freshly synthesized (a) and after cycling degradation (b).

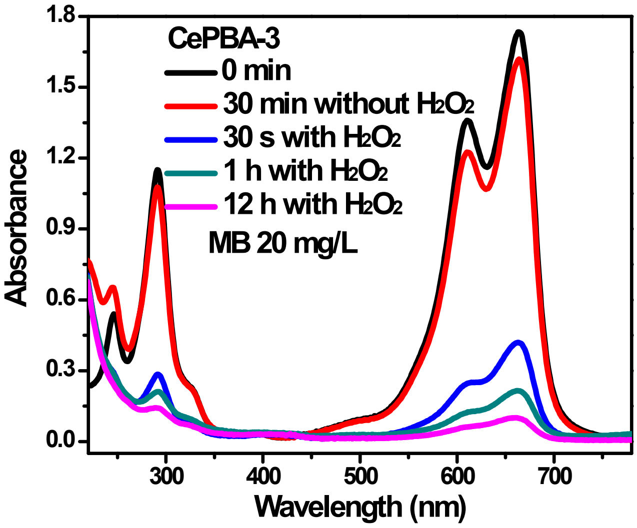

Fig. S21 The degradation performance of CePBA-3 with large particle size toward MB aqueous solution with the concentration of 20 mg/L.